Correlated Dynamics of the Motion of Proton-Hole Wave Packets in a Photoionized Water Cluster

Zheng Li (李铮),[1,2] Mohamed El-Amine Madjet,[1] Oriol Vendrell,[1,*] and Robin Santra[1,2]
[1]*Center for Free-Electron Laser Science, DESY, Notkestrasse 85, D-22607 Hamburg, Germany*
[2]*Department of Physics, University of Hamburg, D-20355 Hamburg, Germany*
(Received 3 September 2012; published 15 January 2013)

We explore the correlated dynamics of an electron hole and a proton after ionization of a protonated water cluster by extreme ultraviolet light. An ultrafast decay mechanism is found in which the proton-hole dynamics after the ionization are driven by electrostatic repulsion and involve a strong coupling between the nuclear and electronic degrees of freedom. We describe the system by a quantum-dynamical approach and show that nonadiabatic effects are a key element of the mechanism by which electron and proton repel each other and become localized at opposite sides of the cluster. Based on the generality of the decay mechanism, similar effects may be expected for other ionized systems featuring hydrogen bonds.

DOI: 10.1103/PhysRevLett.110.038302 PACS numbers: 82.20.Gk, 31.50.Gh, 33.80.Eh, 82.33.Fg

Correlated motions of electrons and protons in the so-called proton coupled electron transfer reactions play a crucial role in charge transfer processes in a range of biological, chemical, and material science scenarios and have been the subject of intensive study over many years [1–3]. These reactions can be thermally activated processes occurring on relatively long time scales, in which the reorganization of the molecular environment plays a decisive role [1,2], as well as ultrafast proton coupled electron transfer processes occurring upon photoexcitation [4]. Some examples include the relaxation of electron vacancies in DNA and in crystals made of DNA bases, which are known to proceed via correlated proton and electron transfer reactions occurring in ps time scales [5,6]. Proton transfer processes triggered by a sudden change in electronic structure are also known to protect DNA base pairs from photodamage caused by UV-visible light absorption and mediate the decay back to the ground electronic state [7]. Nonadiabatic effects, in which the nuclear motion strongly couples to the evolution of the electrons, are ubiquitous in the kind of processes described above.

The response of matter to ionizing extreme ultraviolet (XUV) radiation in the range 20–100 eV has been the subject of much interest in recent years due to opportunities offered by the generation of very short pulses in this energy range, opening the door to time-resolved studies of the induced ultrafast dynamics in the fs time regime [8–15]. The ionization from outer-valence shells can induce an ultrafast rearrangement of the electronic cloud in what are referred to as hole migration processes [16,17]. The increased total charge and the modified bonding structure of a sample may result in changes in its nuclear configuration possibly reaching structures of strong nonadiabatic mixing between electronic states. Examples of ultrafast nuclear dynamics involving hydrogen atoms after XUV photoionization are known and have been measured by pump-probe techniques at the Free Electron Laser at Hamburg (FLASH) [8]. The fragmentation of protonated water clusters $H(H_2O)_n^+$ after XUV irradiation and removal of an outer-valence electron was recently measured at FLASH. The fragmentation products and their kinetic energies were recorded [18,19]. Systems in which a proton, and thereby an extra positive charge, is supported by a number of hydrogen-bonded molecules, are ubiquitous in soft condensed matter such as water [20] or in proton-exchange membranes such as those used in fuel cell applications [21], where they mediate charge transport. A time-resolved picture and most mechanistic details of the nuclear-electronic dynamics after their ionization are, however, not yet known.

Here, we investigate the decay and relaxation mechanism of the electron-hole generated by absorption of XUV radiation in a prototypical water cluster, the so-called Zundel cation, $H(H_2O)_2^+$. We find an ultrafast coupled proton-hole relaxation process operating after photoionization from the outer-valence shell. The correlation function between the location of proton and hole shows that they respond to each other within few fs and quickly separate irreversibly. This is a consequence of the strong electrostatic repulsion between them, which results in potential energy surfaces (PES) for the nuclear motion with large gradients, but this is not the whole picture. As discussed below, strong nonadiabatic effects involving the breakdown of the Born-Oppenheimer approximation play a crucial role in the relaxation mechanism. The fact that PES topologies are to a large extent related to the electrostatic repulsion between the hole and the proton indicates a general class of vibrational-electronic decay mechanisms operating in ionized hydrogen-bonded systems that should thereby be quite insensitive to particular details of their molecular and electronic structure.

The PES of the three lowest-energy states of the dication are shown in Fig. 1(a). They were calculated at the complete active space self-consistent field level of theory [22] with the MOLCAS suite of programs [23]. The two nuclear coordinates of the 2D cut in Fig. 1(a) correspond to the

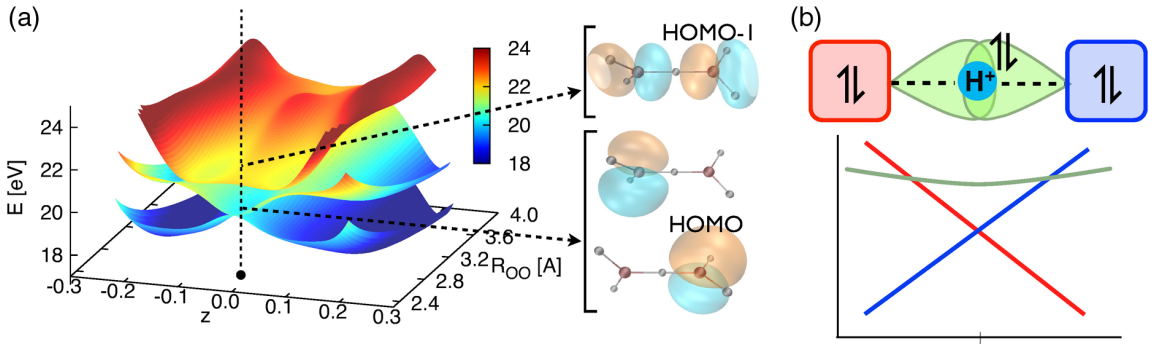

FIG. 1 (color online). (a) Potential energy surfaces of the three lowest electronic states of $H(H_2O)_2^{++}$ for the z (central proton position projected onto the oxygen-oxygen axis) and R (oxygen-oxygen distance) coordinates and keeping the rest of the vibrational modes frozen. The dot marks the Frank-Condon nuclear geometry. The orbitals shown represent the highest occupied molecular orbitals at the Hartree-Fock mean field level, and they correspond to the electron hole in the leading configuration for each of the three lowest-energy electronic states of the dication in a multiconfigurational description. (b) Scheme of the hydrogen-bonded system indicating the location of the electron pairs that can be ionized and the corresponding potential energy surfaces as a function of the central proton position. Ionization leading to the electronic states under consideration can take place from lone electron pairs on each monomer (in red and blue, negative and positive slope curves, respectively) or from the electrons involved in the hydrogen bonding (in green, horizontal curve).

oxygen-oxygen distance (R) and to the projection of the central proton position onto the oxygen-oxygen axis (z), whereas the rest of the coordinates are held fixed. A schematic representation of the vibrational coordinates may be found in Fig. 2. The point in coordinate space marked with a dot signals the position of the minimum energy configuration in the ground electronic state of $H(H_2O)_2^+$. Therefore, the nuclear wave packet is centered at this position immediately after photoionization. At such geometry of the cluster the two lowest electronic states of the dication are energetically degenerate [24]. The orbitals shown in Fig. 1(a) indicate the electron hole in a 1-particle picture. The electronic configurations with the missing electron in such orbitals contribute to more than 90% in the respective multiconfigurational electronic wave functions, indicating that a 1-particle picture description of the states under consideration is adequate in this case. By inspecting them we realize that the two lowest-energy states can be described as removing an electron from a lone electron pair in either water molecule.

The topology of the three low lying PES of the dication is illustrated schematically in Fig. 1(b) as a function of the central proton position. The shape of the PES is mostly the result of the electrostatic repulsion between the positive charge density associated with the central proton and that of the electron hole. This is made clear by noting that the gradient of the PES at the central point of conical intersection is about 6.5 eV · Å^{-1}. This is equivalent to two point charges of equal sign at a distance of 1.4 Å; the distance of the central proton to one of the oxygen atoms is about 1.2 Å at the equilibrium geometry of the cluster. When the central proton is displaced towards, e.g., the water molecule on the left, the electronic state with the hole on the water molecule on the right side stabilizes, while the state with the hole on the left side destabilizes, resulting in the conical intersection between the electronic states as a function of the proton position. The third electronic state of the dication can be described by an electron hole delocalized mostly around the central proton. Therefore, the PES is quite flat along the proton transfer coordinate in the vicinity of the Franck-Condon point. When the proton is displaced towards either water molecule, however, the electron hole eventually becomes more stable on a localized water site, and at that geometry the third dicationic state crosses with the second one, resulting also in a seam of conical intersection.

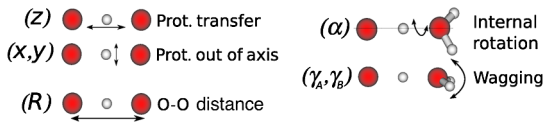

FIG. 2 (color online). Schematic representation of the seven internal nuclear coordinates used in the wave packet propagations showing in each case the relevant atoms. The proton transfer coordinate used in this work was transformed as $z' = z/(R - \delta)$ [28], where δ is a constant. In this work appearances of (z) refer to the (z') defined here.

The ultrafast dynamics of the protonated water dimer unfolding after outer-valence ionization were computed quantum dynamically using the Heidelberg implementation [25] of the multiconfiguration time-dependent Hartree method [26,27]. Out of the total $3N_a - 6 = 15$ vibrational coordinates of the system, where N_a equals the number of atoms in the system, seven were kept active for the dynamics calculations and the other eight were kept frozen at their ground state equilibrium values. The active vibrational modes are shown in Fig. 2 and correspond to the three Cartesian coordinates locating the central proton in the frame defined by the water molecules, the oxygen-oxygen

distance, the water molecule wagging modes, and the relative angle between both water molecules around the axis connecting both oxygen atoms. The remaining frozen coordinates correspond to the internal degrees of freedom of each monomer, which are considered as rigid bodies, and the two rocking angles. The separation in active and inactive modes is made based on the vibrational frequencies of the involved motions. Higher frequency modes are kept frozen, since they are expected to be less coupled to the geometric rearrangements after ionization. A detailed description of the coordinates used and of the kinetic energy operator in this set of internal coordinates may be found in Ref. [28].

The Hamiltonian of the system in diabatic representation reads [29]

$$\hat{H} = \hat{T}_n \otimes \hat{\mathbf{1}}_d + \sum_{i,j} |i\rangle \hat{W}_{i,j}(\mathbf{Q}) \langle j|, \tag{1}$$

where $\hat{W}_{ij}$ operates on the space of the vibrational degrees of freedom, $\hat{\mathbf{1}}_d = \sum_i |i\rangle\langle i|$ is the unit operator in the discrete space of the diabatic electronic states, and $|i\rangle$ refers to the ith diabatic electronic state. The diabatization procedure used is based on regularized diabatic states [30] and details will be presented elsewhere. After ionization, assuming a sudden electron ejection that leaves the system in the ith electronic state, the corresponding wave packet is $\Psi_i(t=0) = \Phi_0(\mathbf{Q}) \otimes |i\rangle$. The nuclear part $\Phi_0(\mathbf{Q})$ corresponds to the ground vibrational state on the ground electronic state PES of $H(H_2O)_2^+$. Such wave packets are propagated for every initial electronic state in coupled PES using the Hamiltonian in Eq. (1). We assume the ionization cross section to be constant over the considered energy range for the initial electronic states. Therefore, the observables calculated from each propagation are averaged with equal weight.

The ultrafast correlated dynamics of hole and proton are made explicit by inspecting the correlation function between their positions, shown in Fig. 3. The correlation function is defined as $C_{ph} = S_{ph}/\sqrt{S_{pp}S_{hh}}$, with $S_{xy} = \langle \hat{x}\,\hat{y}\rangle - \langle \hat{x}\rangle\langle \hat{y}\rangle$. C_{ph} is bound to take values between -1, complete anticorrelation, and $+1$, complete correlation. For the excess proton position operator we simply take $\hat{z}$, the projection of the central proton position onto the oxygen-oxygen axis of the cluster. A convenient definition of the hole position operator that can be readily applied to the propagated wave packet is

$$\hat{h} = \frac{1}{2}\hat{R} \otimes (|r\rangle\langle r| - |l\rangle\langle l|), \tag{2}$$

where $|l\rangle$ and $|r\rangle$ refer to the two diabatic electronic states with the hole localized on the left-hand and on the right-hand side water monomers, respectively, and $\hat{R}$ is the position operator corresponding to the oxygen-oxygen distance. According to this definition, the average location of the electron hole corresponds to the position of the left (right) oxygen atom when the system is in the electronic state $|l\rangle$ ($|r\rangle$). The correlation function in Fig. 3 is obtained by summing over the different initially populated electronic states. At $t = 0$ the proton and hole positions are still uncorrelated. The degree of anticorrelation increases very quickly as the proton is displaced towards one of the water monomers and the hole moves in the opposite direction, reaching almost -1 in about 5 fs. A small recurrence in the correlation function is seen between 7 and 11 fs. It originates from the bounceback motion of the proton against the water monomers, which have practically not yet started moving simply due to their higher inertia. After 10–20 fs proton and hole have irreversibly localized at opposite sides of the system, although the average oxygen-oxygen distance has only increased by 0.2 Å and larger recurrences could be expected. This irreversibility is a direct consequence of the multidimensional nature of the triggered vibrational-electronic motion, which prevents the wave packet, just a few fs after photoexcitation, from returning to nuclear and electronic configurations resembling the initially uncorrelated state.

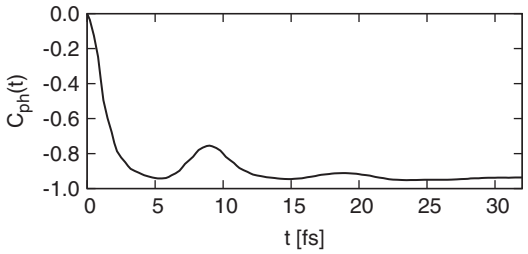

FIG. 3. Correlation function between proton and electron-hole positions obtained from the propagated wave packet.

The ultrafast nuclear dynamics and fragmentation after ionization are shown in Figs. 4(a)–4(c), which illustrate the dynamics of the cluster in the z, R coordinates after integration over all other nuclear coordinates and electronic states. As the proton and hole quickly separate, the central proton approaches the vicinity of an oxygen atom in less than 5 fs. At about 10 fs there is a revival in which the proton bounces back to the center of the cluster because, as already mentioned, the oxygen atoms did not yet have time to move. After 15 fs the oxygen atoms have already separated by about 0.2 Å, and the probability that the proton is found at the central position between the water molecules has almost vanished. At this point, the correlated dynamics between the proton and the electron hole are over and they are found localized at opposite sites of the cluster, leading to fragmentation of the system with 100% probability.

In order to illustrate the dramatic role of the nonadiabatic coupling between nuclear motion and electron-hole dynamics, we briefly discuss the quantum dynamics of the dication upon ionization in the adiabatic representation but neglecting the nonadiabatic coupling altogether. Therefore, the wave packets evolve in uncoupled Born-Oppenheimer PES of the ionized system, and the uncoupled Hamiltonian operator reads

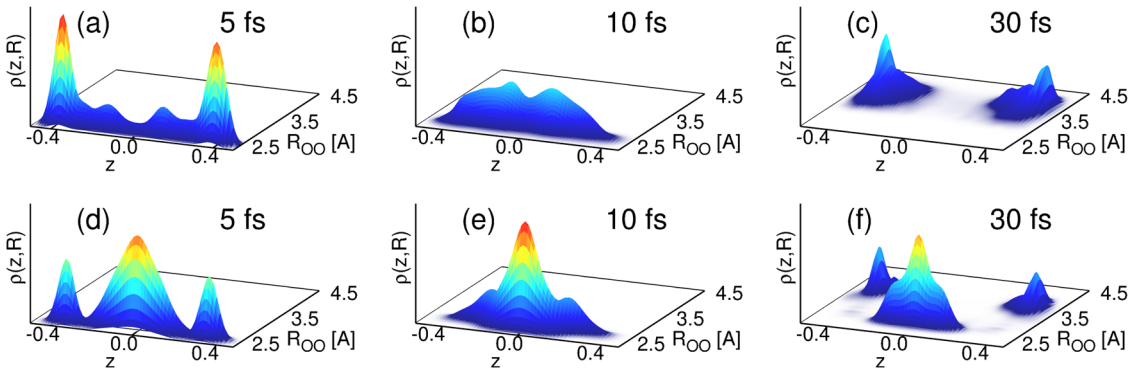

FIG. 4 (color online). Reduced probability densities in the z (central proton position projected onto the oxygen-oxygen axis) and R (oxygen-oxygen distance) coordinates obtained from the propagated wave packets after tracing over all other vibrational modes and electronic states. Snapshots (a)–(c) correspond to propagations with the full Hamiltonian in Eq. (1). Snapshots (d)–(f) correspond to propagation without nonadiabatic coupling in the Hamiltonian, Eq. (3).

$$\hat{H} = \hat{T}_n \otimes \hat{\mathbf{1}}_a + \sum_\alpha |\alpha\rangle \hat{V}_\alpha(\mathbf{Q}) \langle\alpha|, \tag{3}$$

where $\hat{\mathbf{1}}_a = \sum_\alpha |\alpha\rangle\langle\alpha|$ and $|\alpha\rangle$ are now uncoupled adiabatic electronic states. The reduced probability density $\rho(z, R)$ in which all other nuclear coordinates and electronic states are integrated over is shown for this case in Figs. 4(d)–4(f). The part of the initial wave packet on the ground electronic state PES of the dication, i.e., initially below the lowest energy conical intersection, escapes from the Franck-Condon region in about 5–10 fs, quickly leading to the dissociation channel $H_3O^+ + H_2O^+$. The reason is that in the lowest adiabatic electronic state of the dication, the central proton and electron hole are always at opposite sides of the cluster (cf. Fig. 1). This is not the case when the nuclear dynamics start in the two lowest excited states of the dication. Although the cluster is doubly charged, the missing coupling between nuclei and electrons prevents it from fragmenting, the electron hole and proton cannot rearrange and the system stays bound. This is clearly seen by comparing Figs. 4(a) and 4(d). It is worth mentioning at this point that the fragmentation experiments in Ref. [18] do not report unfragmented clusters after ionization.

In conclusion, we have described an ultrafast decay and relaxation mechanism by which an outer-valence hole generated by XUV light in a strongly hydrogen-bonded system triggers proton-hole correlated dynamics unfolding in a time scale of just a few fs. The motion of the proton and the hole is anticorrelated and strongly coupled and their dynamics are driven by their electrostatic repulsion, which results in PESs with large relative gradients at regions of intersection and strong nonadiabatic effects. The rearrangement of the proton and hole leads to electronic relaxation of the system, indicating that the dynamics of the lightest nuclei is important when considering the motion of electron holes in molecular systems and clusters. Artificially removing the nonadiabatic coupling in our quantum dynamical calculations completely quenches the described mechanism because proton and hole cannot rearrange. The electrostatic nature of the reported mechanism suggests that this class of decay pathway may be a common feature of ionized hydrogen-bonded systems.

We thank the Helmholtz Association for financial support through the Virtual Institute on "Dynamic Pathways in Multidimensional Landscapes."

*oriol.vendrell@cfel.de

[1] R. I. Cukier and D. G. Nocera, Annu. Rev. Phys. Chem. **49**, 337 (1998).
[2] S. Hammes-Schiffer and A. A. Stuchebrukhov, Chem. Rev. **110**, 6939 (2010).
[3] D. R. Weinberg, C. J. Gagliardi, J. F. Hull, C. F. Murphy, C. A. Kent, B. C. Westlake, A. Paul, D. H. Ess, D. G. McCafferty, and T. J. Meyer, Chem. Rev. **112**, 4016 (2012).
[4] B. Li, J. Zhao, K. Onda, K. D. Jordan, J. Yang, and H. Petek, Science **311**, 1436 (2006).
[5] A. Kumar and M. D. Sevilla, Chem. Rev. **110**, 7002 (2010).
[6] A. Krivokapić, J. N. Herak, and E. Sagstuen, J. Phys. Chem. A **112**, 3597 (2008).
[7] A. L. Sobolewski, W. Domcke, and C. Hättig, Proc. Natl. Acad. Sci. U.S.A. **102**, 17903 (2005).
[8] Y. H. Jiang, A. Rudenko, O. Herrwerth, L. Foucar, M. Kurka, K. U. Kühnel, M. Lezius, M. F. Kling, J. van Tilborg, A. Belkacem, K. Ueda, S. Düsterer, R. Treusch, C. D. Schröter, R. Moshammer, and J. Ullrich, Phys. Rev. Lett. **105**, 263002 (2010).
[9] T. Popmintchev, M.-C. Chen, P. Arpin, M. M. Murnane, and H. C. Kapteyn, Nat. Photonics **4**, 822 (2010).
[10] H. Chapman, J. Ullrich, and J. M. Rost, J. Phys. B **43**, 190201 (2010).
[11] M. E. Madjet, O. Vendrell, and R. Santra, Phys. Rev. Lett. **107**, 263002 (2011).
[12] J. P. Farrell, S. Petretti, J. Foerster, B. K. McFarland, L. S. Spector, Y. V. Vanne, P. Decleva, P. H. Bucksbaum, A. Saenz, and M. Guehr, Phys. Rev. Lett. **107**, 083001 (2011).

[13] F. Kelkensberg, W. Siu, J. F. Pérez-Torres, F. Morales, G. Gademann, A. Rouzée, P. Johnsson, M. Lucchini, F. Calegari, J. L. Sanz-Vicario, F. Martín, and M. J. J. Vrakking, Phys. Rev. Lett. **107**, 043002 (2011).

[14] W. Siu, F. Kelkensberg, G. Gademann, A. Rouzee, P. Johnsson, D. Dowek, M. Lucchini, F. Calegari, U. De Giovannini, A. Rubio, R. R. Lucchese, H. Kono, F. Lepine, and M. J. J. Vrakking, Phys. Rev. A **84**, 063412 (2011).

[15] X. Zhou, P. Ranitovic, C. W. Hogle, J. H. D. Eland, H. C. Kapteyn, and M. M. Murnane, Nat. Phys. **8**, 232 (2012).

[16] A. I. Kuleff, J. Breidbach, and L. S. Cederbaum, J. Chem. Phys. **123**, 044111 (2005).

[17] F. Remacle and R. D. Levine, Proc. Natl. Acad. Sci. U.S.A. **103**, 6793 (2006).

[18] L. Lammich, C. Domesle, B. Jordon-Thaden, M. Förstel, T. Arion, T. Lischke, O. Heber, S. Klumpp, M. Martins, N. Guerassimova, R. Treusch, J. Ullrich, U. Hergenhahn, H. B. Pedersen, and A. Wolf, Phys. Rev. Lett. **105**, 253003 (2010).

[19] A. Wolf, H. B. Pedersen, L. Lammich, B. Jordon-Thaden, S. Altevogt, C. Domesle, U. Hergenhahn, M. Förstel, and O. Heber, J. Phys. B **43**, 194007 (2010).

[20] D. Marx, M. Tuckerman, J. Hutter, and M. Parrinello, Nature (London) **397**, 601 (1999).

[21] K.-D. Kreuer, Chem. Mater. **8**, 610 (1996).

[22] J. Olsen, B. O. Roos, P. Jørgensen, and H. J. A. Jensen, J. Chem. Phys. **89**, 2185 (1988).

[23] V. Veryazov, P.-O. Widmark, L. Serrano-Andrés, R. Lindh, and B. O. Roos, Int. J. Quantum Chem. **100**, 626 (2004).

[24] The two lowest electronic states of the dication belong to the E irreducible representation within the D_{2d} symmetry point group, which is adequate to classify the electronic states of the system at the Frank-Condon point.

[25] H.-D. Meyer, G. A. Worth, M. H. Beck, A. Jäckle, M.-C. Heitz, S. Wefing, U. Manthe, S. Sukiasyan, A. Raab, M. Ehara, C. Cattarius, F. Gatti, F. Otto, M. Nest, A. Markmann, M. R. Brill, and O. Vendrell, The MCTDH Package, Version 8.4, 2007, http://mctdh.uni-hd.de.

[26] H.-D. Meyer, U. Manthe, and L. S. Cederbaum, Chem. Phys. Lett. **165**, 73 (1990).

[27] M. H. Beck, A. Jäckle, G. A. Worth, and H.-D. Meyer, Phys. Rep. **324**, 1 (2000).

[28] O. Vendrell, M. Brill, F. Gatti, D. Lauvergnat, and H.-D. Meyer, J. Chem. Phys. **130**, 234305 (2009).

[29] G. A. Worth and L. S. Cederbaum, Annu. Rev. Phys. Chem. **55**, 127 (2004).

[30] H. Köppel, J. Gronki, and S. Mahapatra, J. Chem. Phys. **115**, 2377 (2001).